

Supporting Information

Designing luminescent diimine-Cu (I)-phosphine complexes by tuning N-ligand counteranions: correlation of weak interactions, luminescence and THz absorption spectra

Zhen-Zhou Sun, †^a Ning Zhu, †^a Xun Pan, ^a Guo Wang, ^a Yu-Ping Yang, ^b Qi-Ming

Qiu, ^c Zhong-Feng Li, ^a Xiu-Lan Xin, ^d Jian-Ming Liu, ^e Xiao-Qi Li, ^a Qiong-Hua Jin,

**^{a,f} Zhi-Gang Ren, *^g and Qing-Li Zhou, *^h*

^a Department of Chemistry, Capital Normal University, Beijing 100048, China, E-mail:

jinqh@cnu.edu.cn, jinqh204@163.com

^b School of Science, Minzu University of China, Beijing 100081, China

^c School of Science, China University of Geosciences, Beijing 100083, China, E-mail:

qiuqiming890521@163.com

^d School of Light Industry, Beijing Technology and Business University, Beijing 100048, China

^e School of Mathematical Sciences, Peking University, Beijing 100871, China

^f State Key Laboratory of Structural Chemistry Fujian Institute of Research on the Structure of Matter, Chinese Academy of Science Fuzhou, Fujian 350002, China

^g College of Chemistry, Chemical Engineering and Materials Science, Soochow University, Suzhou 215123, China, E-mail: renzhigang@suda.edu.cn

^h Key Laboratory of Terahertz Optoelectronics, Ministry of Education, and Beijing Advanced Innovation Center for Imaging Theory and Technology, Department of Physics, Capital Normal University, Beijing 100048, China, E-mail: qlzhou@cnu.edu.cn

Table of Contents

Fig. S1. The PXRD patterns for complex **1**: simulated from single crystal data (Black) and single-phase polycrystalline sample (Red).

Fig. S2. The PXRD patterns for complex **2**: simulated from single crystal data (Black) and single-phase polycrystalline sample (Red).

Fig. S3. The PXRD patterns for complex **3**: simulated from single crystal data (Black) and single-phase polycrystalline sample (Red).

Fig. S4. The PXRD patterns for complex **4**: simulated from single crystal data (Black) and single-phase polycrystalline sample (Red).

Fig. S5. The PXRD patterns for complex **5**: simulated from single crystal data (Black) and single-phase polycrystalline sample (Red).

Fig. S6. The PXRD patterns for complex **6**: simulated from single crystal data (Black) and single-phase polycrystalline sample (Red).

Fig. S7. Thermal stability curves for complexes **1, 2, 3, 5**.

Fig. S8. Coordination environment of Cu(I) for **1**. Thermal ellipsoids drawn at the 30% probability level. All hydrogen atoms are omitted for clarity.

Fig. S9. Coordination environment of Cu(I) for **2**. Thermal ellipsoids drawn at the 30% probability

level. All hydrogen atoms and solvent molecules are omitted for clarity.

Fig. S10. Coordination environment of Cu(I) for **3**. Thermal ellipsoids drawn at the 30% probability level. All hydrogen atoms are omitted for clarity.

Fig. S11. Coordination environment of Cu(I) for **4**. Thermal ellipsoids drawn at the 30% probability level. All hydrogen atoms are omitted for clarity.

Fig. S12. Coordination environment of Cu(I) for **5**. Thermal ellipsoids drawn at the 30% probability level. All hydrogen atoms are omitted for clarity.

Fig. S13. Coordination environment of Cu(I) for **6**. Thermal ellipsoids drawn at the 30% probability level. All hydrogen atoms are omitted for clarity.

Fig. S14. Weak hydrogen bonds in **3**, including C-H \cdots F bonds (C2-H2 \cdots F1ⁱ, 2.44 Å, C19-H19 \cdots F4ⁱⁱ, 2.41 Å, C20-H20B \cdots F3ⁱⁱⁱ, 2.47 Å, C33-H33A \cdots F4ⁱⁱⁱ, 2.52 Å, C35-H35 \cdots F3ⁱⁱⁱ, 2.49 Å, C42-H42 \cdots F2, 2.40 Å, Symmetric codes: ⁱ 1/2-x, 1/2-y, 1/2-z; ⁱⁱ 1-x, 1-y, 1-z; ⁱⁱⁱ x, -1+y, z).

Fig. S15. Weak hydrogen bonds in **4**, including C-H \cdots O bonds (C9-H9 \cdots O4ⁱ, 2.50 Å, C17-H17 \cdots O1ⁱⁱ, 2.46 Å, C20-H20A \cdots O2, 2.54 Å, C33-H33B \cdots O1, 2.54 Å, C36-H36 \cdots O3ⁱⁱⁱ, 2.44 Å, C45-H45 \cdots O2, 2.57 Å, Symmetric codes: ⁱ 1-x, 1/2+y, 1/2-z; ⁱⁱ 1-x, 1-y, 1-z; ⁱⁱⁱ -1/2+x, 1-y, z).

Fig. S16. Weak hydrogen bonds in **5**, including C-H \cdots F bonds (C1-H1 \cdots F1, 2.32 Å, C3-H3 \cdots F4ⁱ, 2.24 Å, C10-H10 \cdots F2ⁱⁱ, 2.49 Å, C13-H13A \cdots F1, 2.49 Å, C14-H14B \cdots F1, 2.49 Å, C29-H29 \cdots F1ⁱⁱⁱ, 2.53 Å, C34-H34 \cdots F3ⁱⁱ, 2.36 Å, Symmetric codes: ⁱ 2-x, 2-y, 1-z; ⁱⁱ -1+x, y, z; ⁱⁱⁱ 2-x, 1-y, 1-z).

Fig. S17. Weak hydrogen bonds in **6**, including C-H \cdots O bonds (C2-H2B \cdots O2, 2.55 Å, C18-H18 \cdots O1ⁱ, 2.55 Å, C32-H32 \cdots O3ⁱ, 2.53 Å, C39-H39 \cdots O4ⁱⁱ, 2.37 Å, C41-H41 \cdots O2, 2.37 Å, Symmetric codes: ⁱ 1+x, y, z; ⁱⁱ 1-x, 1-y, -z).

Fig. S18. UV-vis absorption spectra for ligands in CH₂Cl₂ at room temperature.

Fig. S19. Solid-state UV-vis spectra for complexes **1-6**.

Table S1. Crystallographic data for **1-6**.

Table S2. Selected bond length (Å) and angles (°) for **1-6**.

Table S3. Intermolecular π - π interactions for complex **1**

Table S4. Intermolecular C-H \cdots π interactions for complex **2**.

Table S5. Intermolecular π - π interactions for complex **3**

Table S6. Intermolecular C-H \cdots π interactions for complex **3**.

Table S7 Hydrogen bonds in asymmetric units for complexes **3**.

Table S8. Intermolecular π - π interactions for complex **4**

Table S9. Intermolecular C-H \cdots π interactions for complex **4**.

Table S10 Hydrogen bonds in asymmetric units for complexes **4**.

Table S11. Intermolecular π - π interactions for complex **5**

Table S12. Intermolecular C-H \cdots π interactions for complex **5**.

Table S13 Hydrogen bonds in asymmetric units for complexes **5**.

Table S14. Intermolecular π - π interactions for complex **6**

Table S15 Hydrogen bonds in asymmetric units for complexes **6**.

Table S16. Energy, oscillator strength and major contribution of the calculated transitions for **1-6**.

Table S17. Calculated molecular frontier orbital energy / eV for **1-6**.

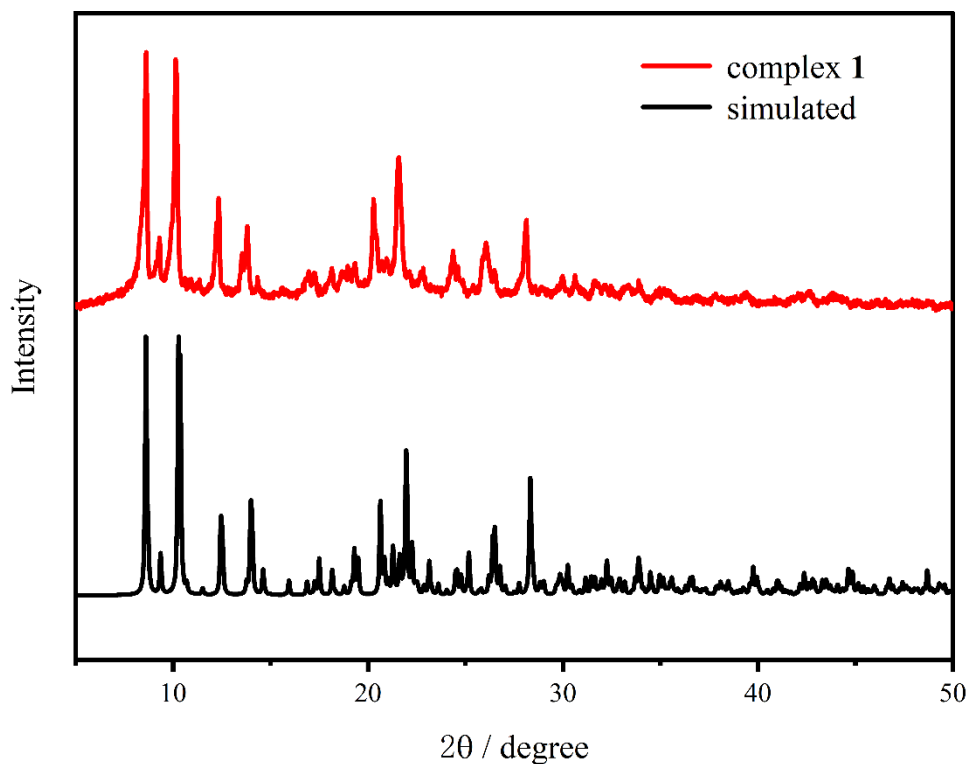


Fig. S1. The PXRD patterns for complex 1: simulated from single crystal data (Black) and single-phase polycrystalline sample (Red).

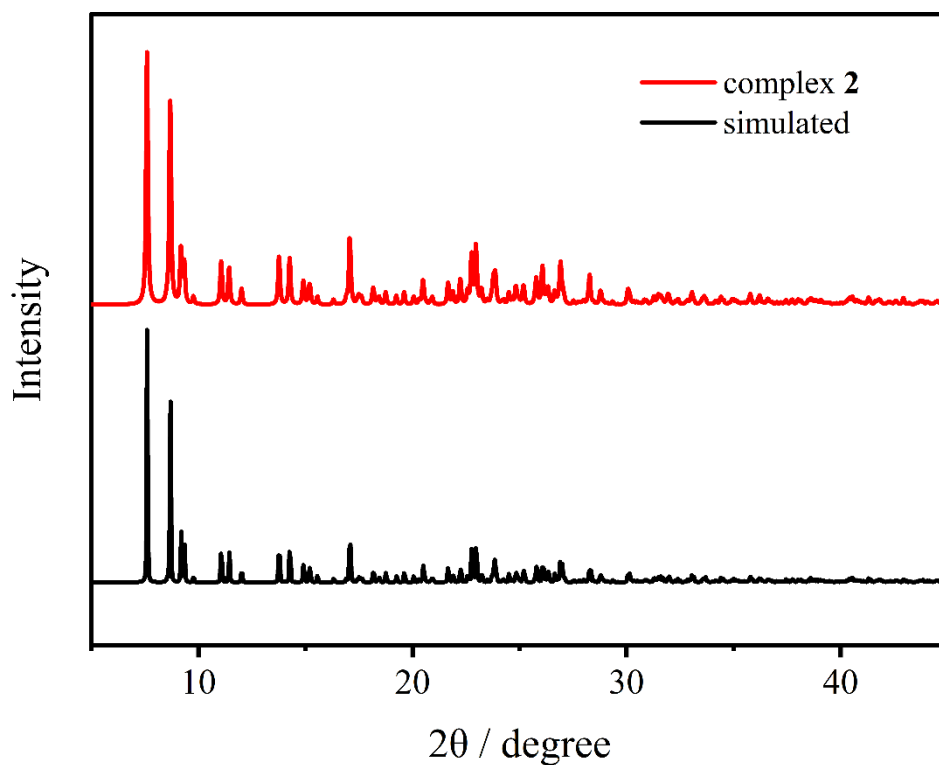


Fig. S2. The PXRD patterns for complex 2: simulated from single crystal data (Black) and single-phase polycrystalline sample (Red).

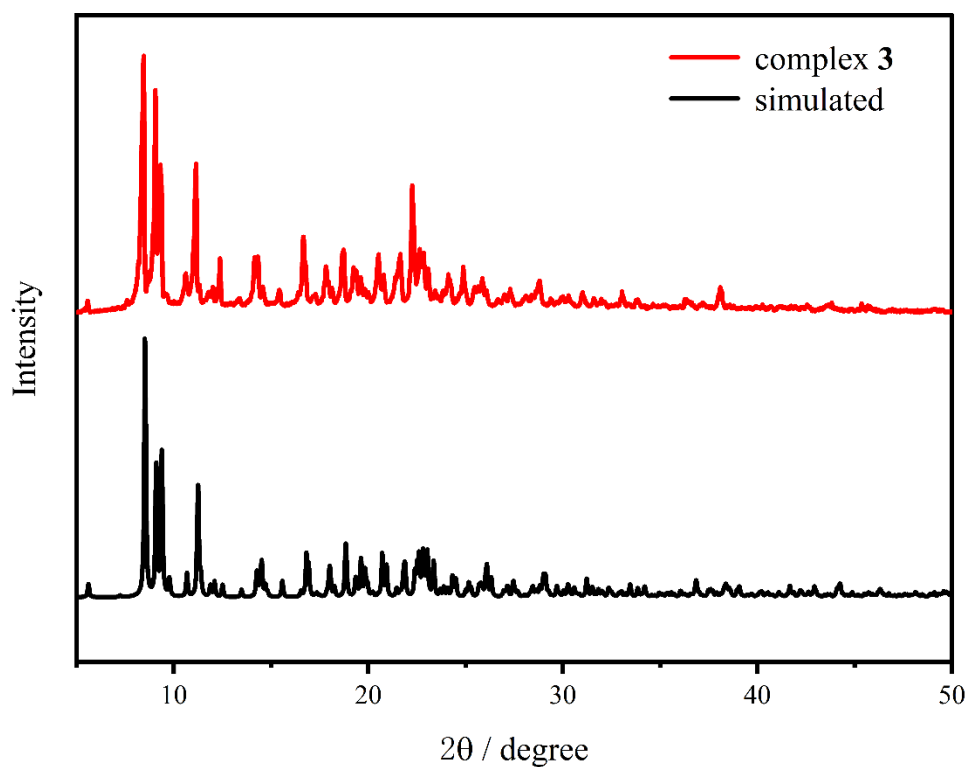


Fig. S3. The PXR D patterns for complex 3: simulated from single crystal data (Black) and single-phase polycrystalline sample (Red).

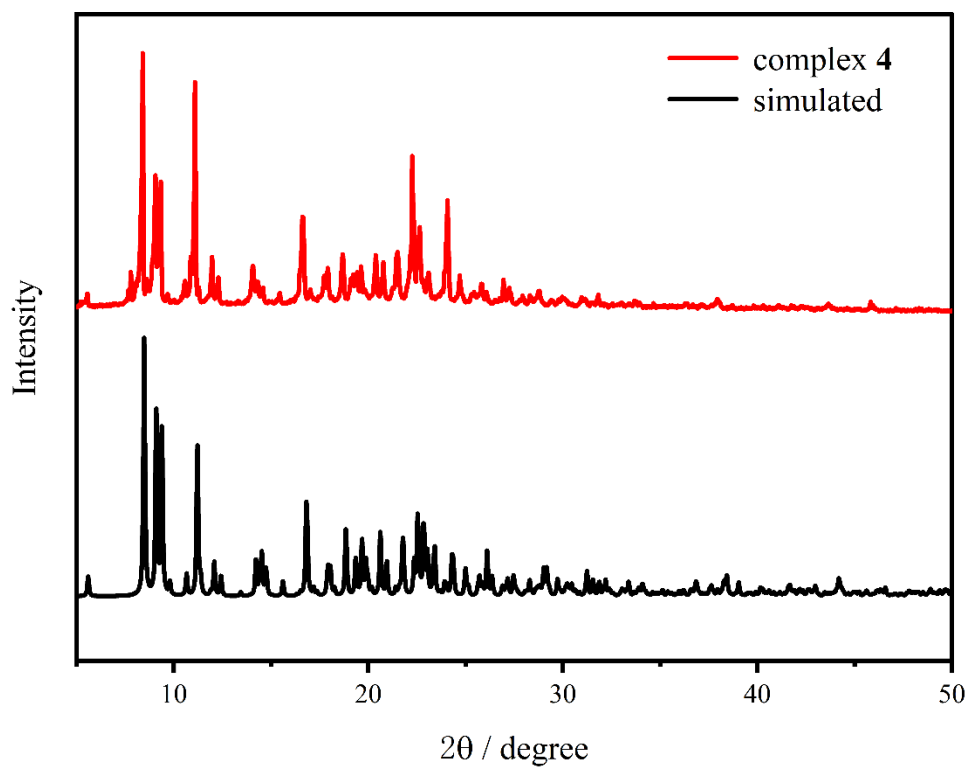


Fig. S4. The PXR D patterns for complex 4: simulated from single crystal data (Black) and single-phase polycrystalline sample (Red).

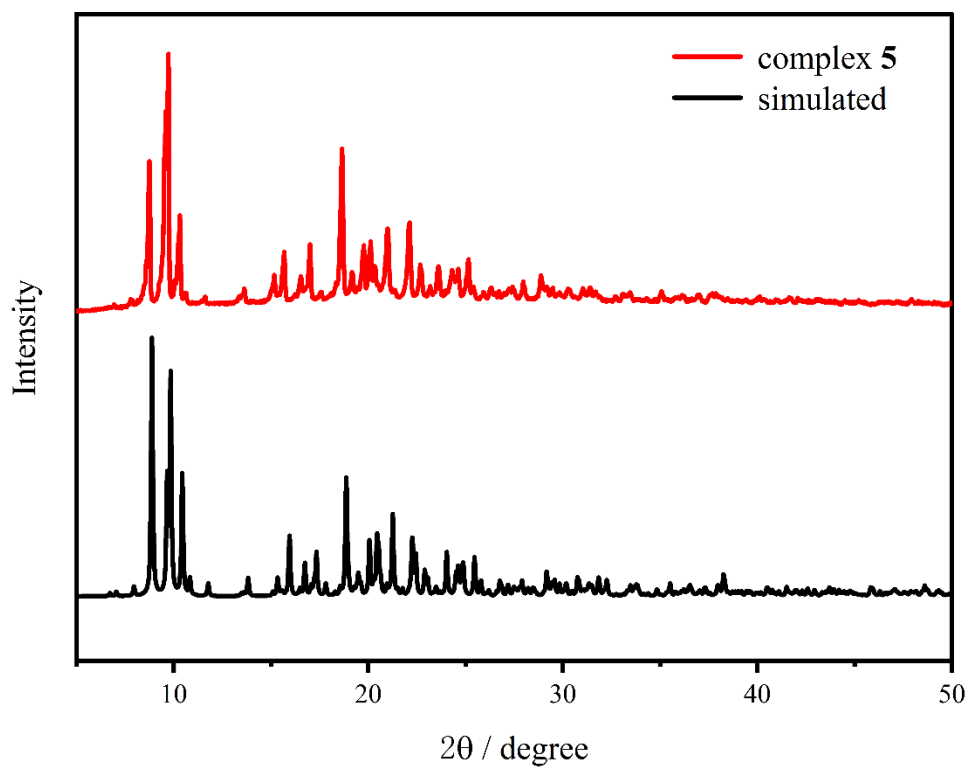


Fig. S5. The PXRd patterns for complex 5: simulated from single crystal data (Black) and single-phase polycrystalline sample (Red).

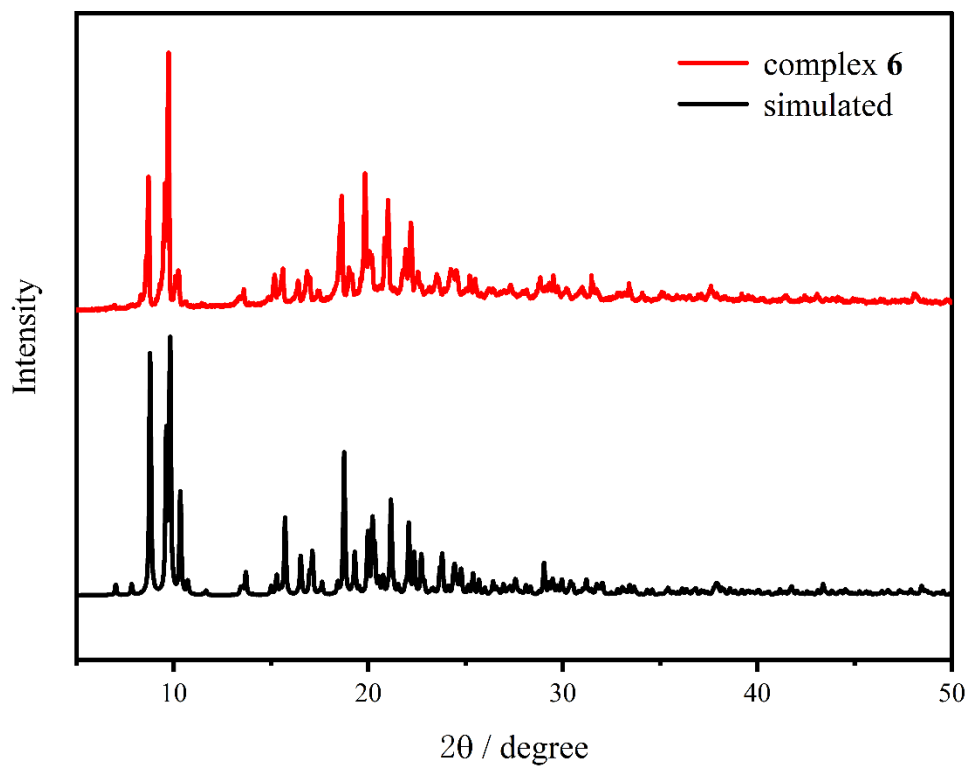


Fig. S6. The PXRd patterns for complex 6: simulated from single crystal data (Black) and single-phase polycrystalline sample (Red).

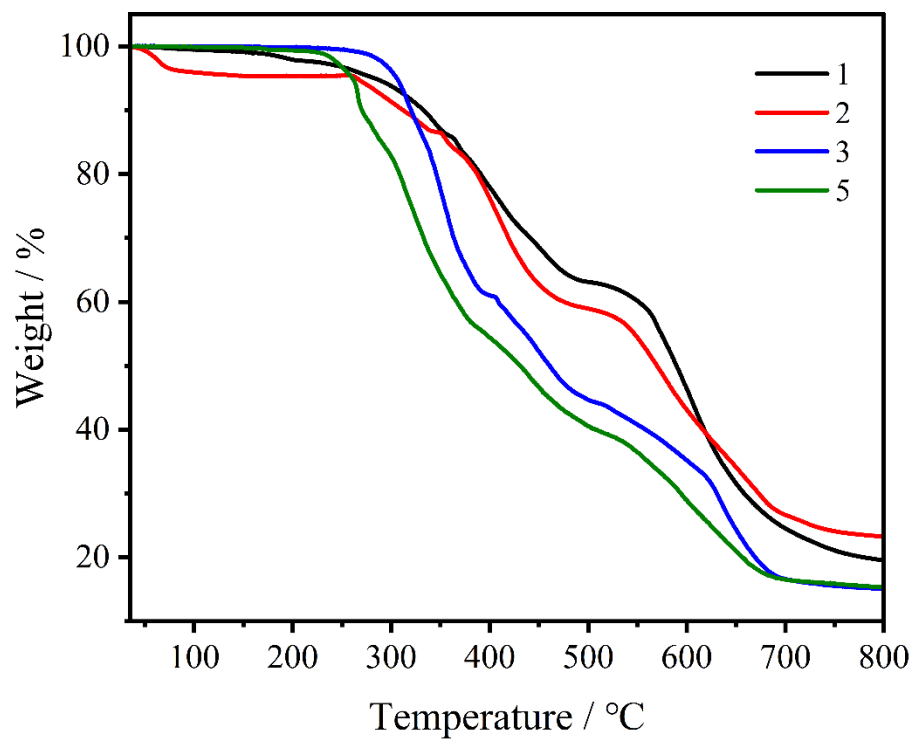


Fig. S7. Thermal stability curves for complexes 1, 2, 3, 5.

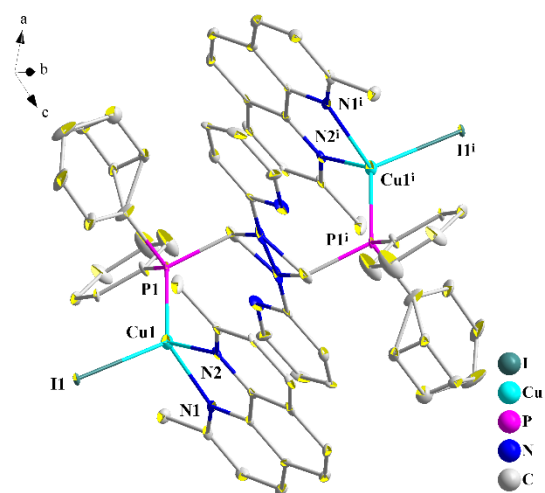


Fig. S8. Coordination environment of Cu(I) for **1**. Thermal ellipsoids drawn at the 30% probability level. All hydrogen atoms are omitted for clarity Symmetric codes: ⁱ 2-x, 1-y, 1-z.

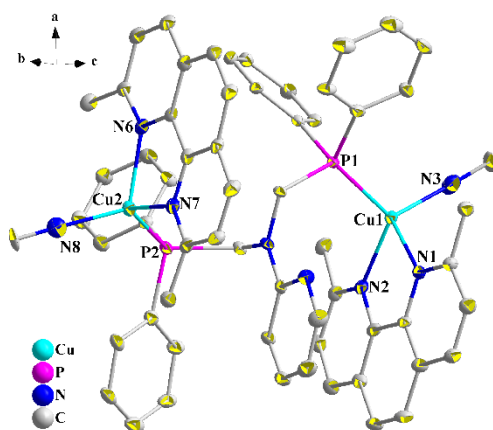


Fig. S9. Coordination environment of Cu(I) for **2**. Thermal ellipsoids drawn at the 30% probability level. All hydrogen atoms and solvent molecules are omitted for clarity.

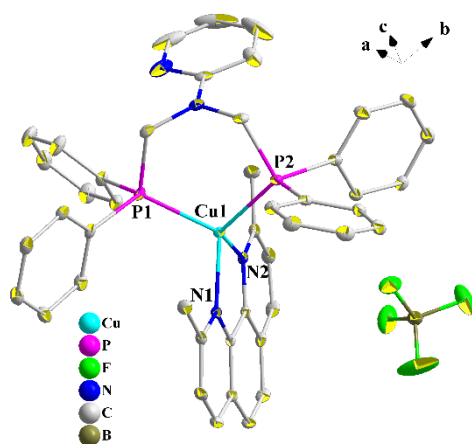


Fig. S10. Coordination environment of Cu(I) for **3**. Thermal ellipsoids drawn at the 30% probability level. All hydrogen atoms are omitted for clarity.

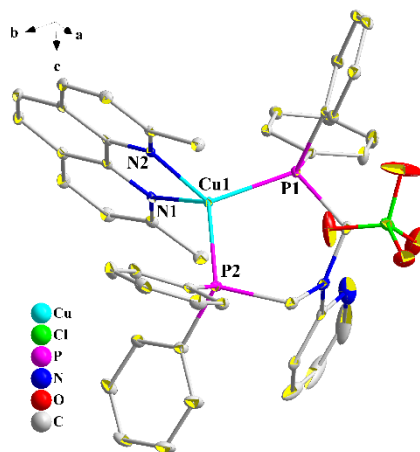


Fig. S11. Coordination environment of Cu(I) for **4**. Thermal ellipsoids drawn at the 30% probability level. All hydrogen atoms are omitted for clarity.

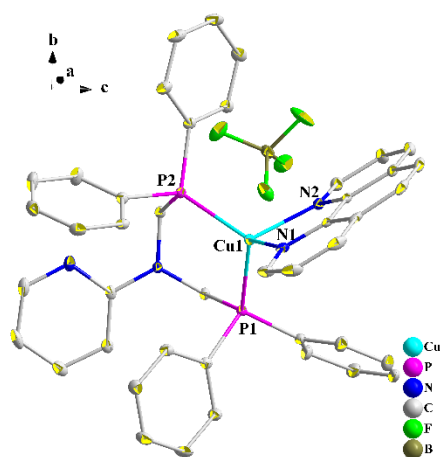


Fig. S12. Coordination environment of Cu(I) for **5**. Thermal ellipsoids drawn at the 30% probability level. All hydrogen atoms are omitted for clarity.

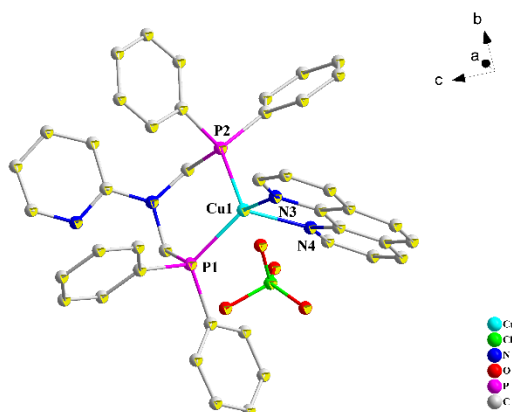


Fig. S13. Coordination environment of Cu(I) for **6**. Thermal ellipsoids drawn at the 30% probability level. All hydrogen atoms are omitted for clarity.

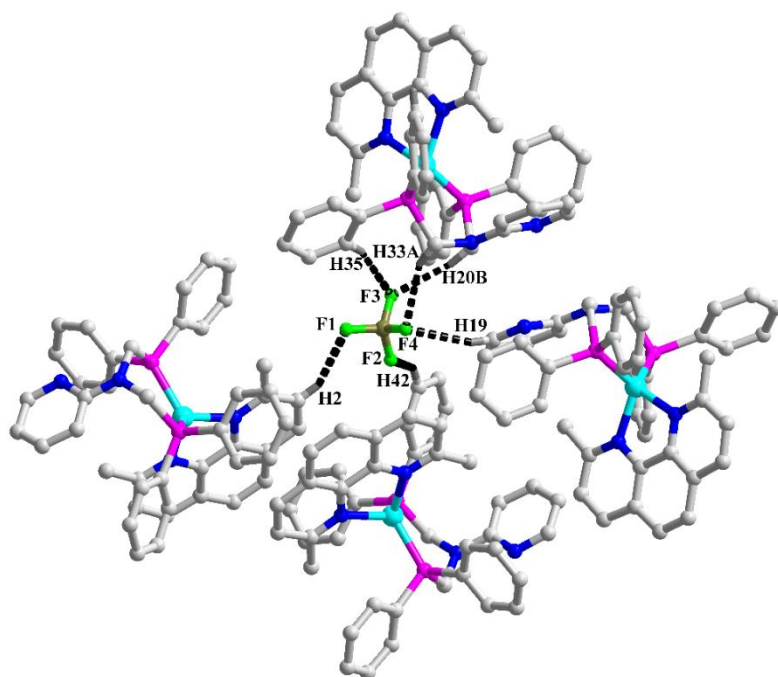


Fig. S14. Weak hydrogen bonds in **3**, including C-H...F bonds (C2-H2...F1ⁱ, 2.44 Å, C19-H19...F4ⁱⁱ, 2.41 Å, C20-H20B...F3ⁱⁱⁱ, 2.47 Å, C33-H33A...F4ⁱⁱⁱ, 2.52 Å, C35-H35...F3ⁱⁱⁱ, 2.49 Å, C42-H42...F2, 2.40 Å, Symmetric codes: ⁱ 1/2-x, 1/2-y, 1/2-z; ⁱⁱ 1-x, 1-y, 1-z; ⁱⁱⁱ x, -1+y, z).

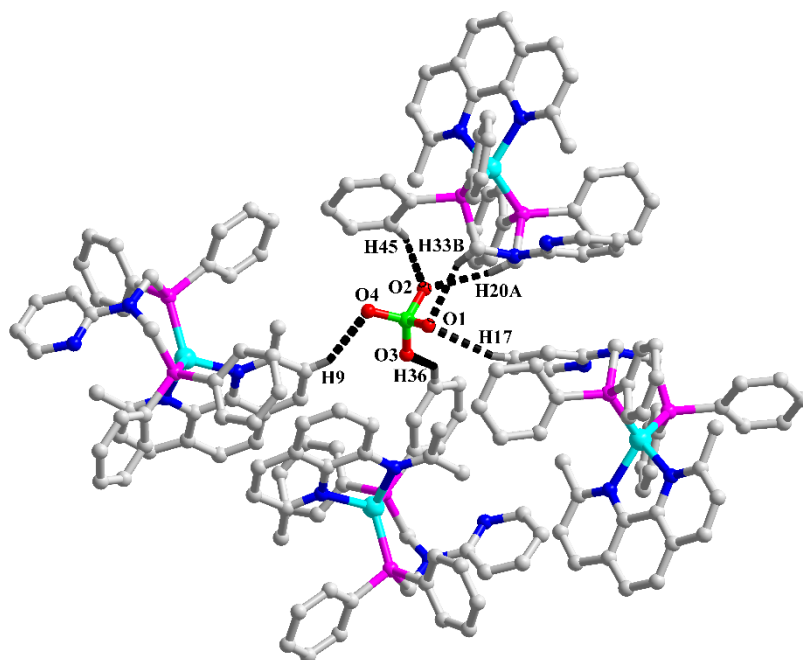


Fig. S15. Weak hydrogen bonds in **4**, including C-H...O bonds (C9-H9...O4ⁱ, 2.50 Å, C17-H17...O1ⁱⁱ, 2.46 Å, C20-H20A...O2, 2.54 Å, C33-H33B...O1, 2.54 Å, C36-H36...O3ⁱⁱⁱ, 2.44 Å, C45-H45...O2, 2.57 Å, Symmetric codes: ⁱ 1-x, 1/2+y, 1/2-z; ⁱⁱ 1-x, 1-y, 1-z; ⁱⁱⁱ -1/2+x, 1-y, z).

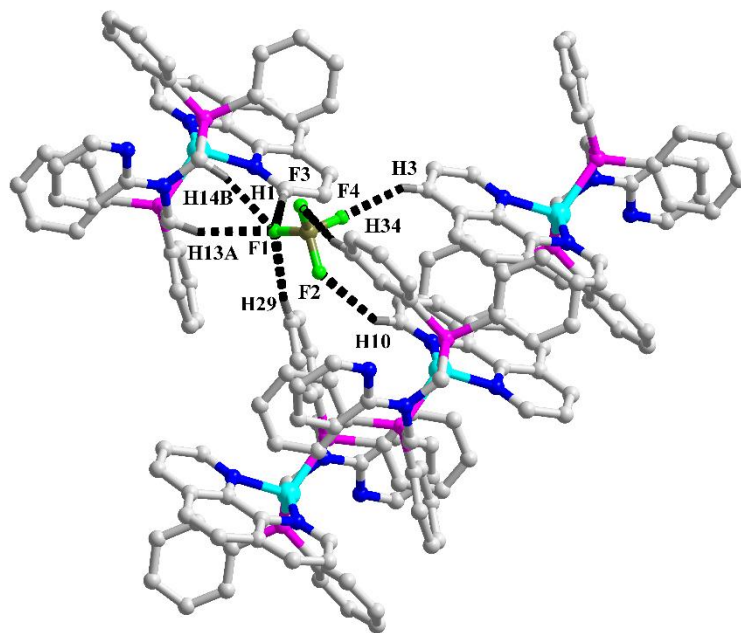


Fig. S16. Weak hydrogen bonds in **5**, including C-H...F bonds (C1-H1...F1, 2.32 Å, C3-H3...F4ⁱ, 2.24 Å, C10-H10...F2ⁱⁱ, 2.49 Å, C13-H13A...F1, 2.49 Å, C14-H14B...F1, 2.49 Å, C29-H29...F1ⁱⁱⁱ, 2.53 Å, C34-H34...F3ⁱⁱ, 2.36 Å, Symmetric codes: ⁱ 2-x, 2-y, 1-z; ⁱⁱ -1+x, y, z; ⁱⁱⁱ 2-x, 1-y, 1-z).

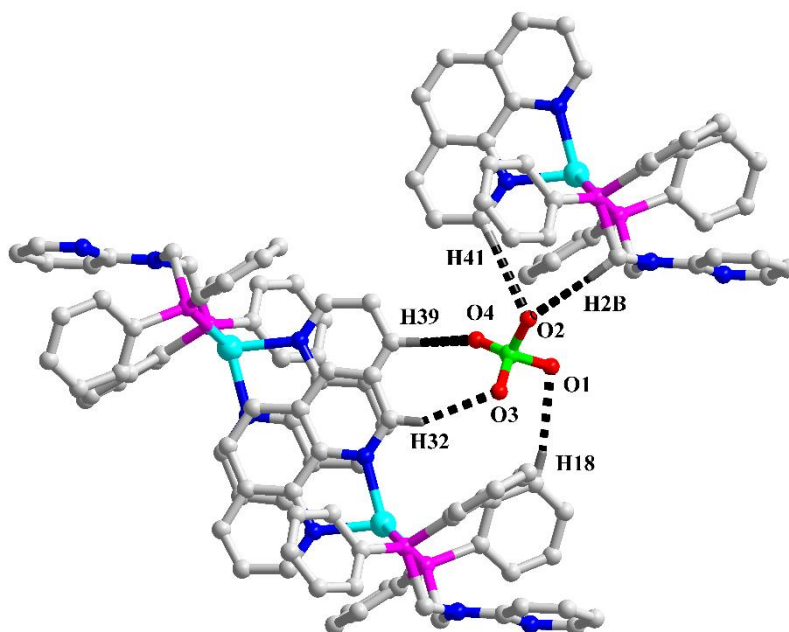


Fig. S17. Weak hydrogen bonds in **6**, including C-H...O bonds (C2-H2B...O2, 2.55 Å, C18-H18...O1ⁱ, 2.55 Å, C32-H32...O3ⁱ, 2.53 Å, C39-H39...O4ⁱⁱ, 2.37 Å, C41-H41...O2, 2.37 Å, Symmetric codes: ⁱ 1+x, y, z; ⁱⁱ 1-x, 1-y, -z).

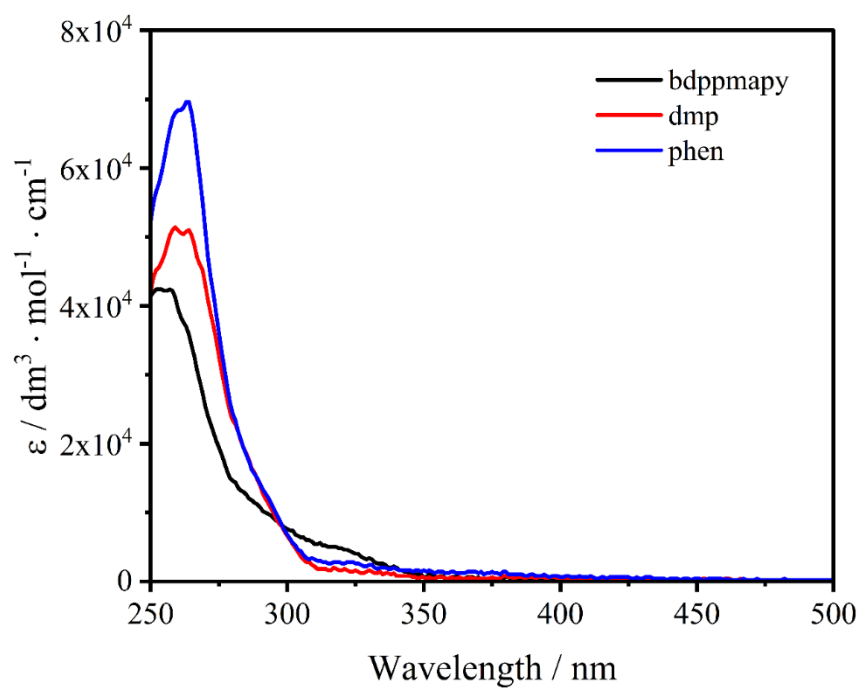


Fig. S18. UV-vis absorption spectra for ligands in CH_2Cl_2 at room temperature.

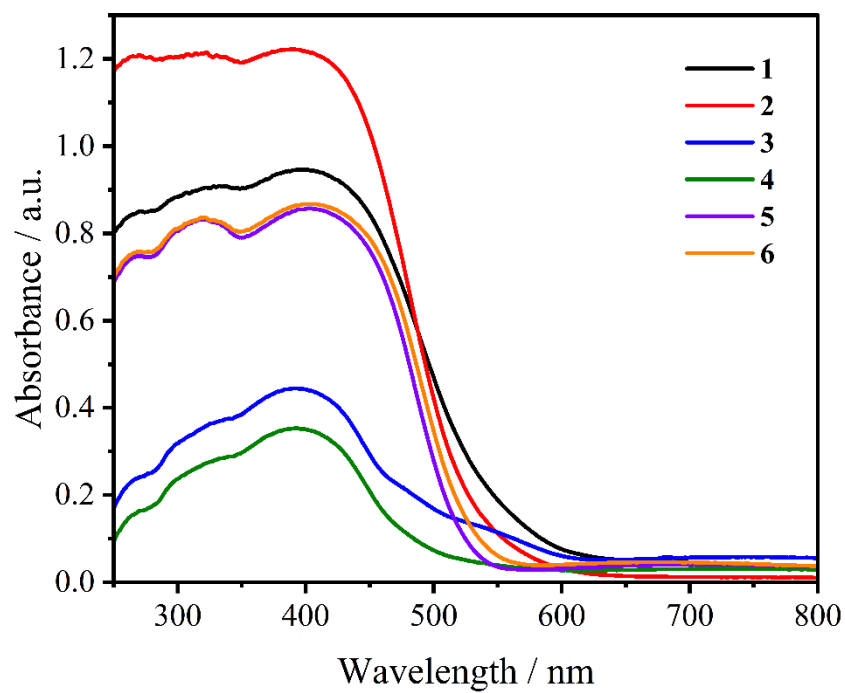


Fig. S19. Solid-state UV-vis spectra for complexes 1-6.

Table S1. Crystallographic data for **1-6**.

Complex	1	2	3	4	5	6
Formula	C ₅₉ H ₅₂ Cu ₂ I ₂ N ₆ P ₂	C ₆₄ H ₆₄ Cu ₂ N ₈ O ₃ P ₂	C ₄₅ H ₄₀ BCu F ₄ N ₄ P ₂	C ₄₅ H ₄₀ ClCuN ₄ O ₄ P ₂	C ₄₃ H ₃₆ BCu F ₄ N ₄ P ₂	C ₄₃ H ₃₆ CuN ₄ P ₂ ClO ₄
Formula weight	1287.88	1182.23	849.10	861.74	821.05	833.85
T / K	100(2)	100(2)	99.99(10)	99.97(10)	106.7	298(2)
Crystal system	Monoclinic	Monoclinic	Monoclinic	Monoclinic	Triclinic	Triclinic
Space group	<i>P</i> 2 ₁ / <i>c</i>	<i>C</i> ₂	<i>I</i> 2/ <i>a</i>	<i>I</i> 2/ <i>a</i>	<i>P</i> $\bar{1}$	<i>P</i> $\bar{1}$
<i>a</i> / Å	12.647(3)	11.7324(2)	24.6200(2)	24.6439(3)	11.5699(5)	11.7400(11)
<i>b</i> / Å	17.053(3)	20.7132(3)	10.20780(9)	10.20305(13)	12.5429(3)	12.5965(13)
<i>c</i> / Å	17.208(3)	23.3587(4)	31.7453(3)	31.8756(4)	13.6715(4)	13.7194(14)
α / (°)	90	90	90	90	88.298(2)	88.186(2)
β / (°)	131.69(3)	95.466(2)	98.0520(9)	98.5114(11)	73.809(3)	73.7570(10)
γ / (°)	90	90	90	90	87.479(3)	87.479(2)
<i>V</i> / Å ³	2771.2(14)	5650.71(16)	7899.46(13)	7926.63(16)	1903.17(12)	1945.6(3)
<i>Z</i>	2	4	8	8	2	2
D _{calc} / g·cm ⁻³	1.543	1.387	1.428	1.444	1.433	1.423
<i>F</i> (000)	1284	2456	3504	3568	844	860
Goodness-of-fit on <i>F</i> ²	1.153	1.059	1.058	1.024	1.038	1.051
<i>R</i> _{int}	0.1453	0.0475	0.0547	0.0371	0.0178	0.0392
<i>R</i> ₁ [<i>I</i> > 2σ(<i>I</i>)] ^[a]	0.0788	0.0827	0.0432	0.0389	0.0290	0.0632
<i>wR</i> ₂ [<i>I</i> > 2σ(<i>I</i>)] ^[b]	0.2015	0.2124	0.1082	0.0947	0.0669	0.1504
<i>R</i> ₁ (all data) ^[a]	0.0802	0.0832	0.0440	0.0407	0.0339	0.0870
<i>wR</i> ₂ (all data) ^[b]	0.2023	0.2129	0.1088	0.0958	0.0698	0.1597
<i>CCDC</i>	2075018	2075019	2075020	2075021	2075022	2075023

$$[a] R = \sum(|F_o| - |F_c|) / \sum|F_o|.$$

$$[b] wR = [\sum w(|F_o|^2 - |F_c|^2)^2 / \sum w(F_o^2)]^{1/2}.$$

Table S2. Selected bond length (Å) and angles (°) for **1-6**.

1			
Cu(1)-I(1)	2.642(2)	P(1)-Cu(1)-I(1)	118.73(8)
Cu(1)-P(1)	2.199(3)	N(1)-Cu(1)-I(1)	107.7(2)
Cu(1)-N(1)	2.091(7)	N(1)-Cu(1)-P(1)	120.0(2)
Cu(1)-N(2)	2.101(7)	N(1)-Cu(1)-N(2)	80.4(3)
		N(2)-Cu(1)-I(1)	101.0(2)
		N(2)-Cu(1)-P(1)	121.9(2)
			Dihedral Angle
		I1-Cu1-P1/N1-Cu1-N2	94.370

2

Cu(1)-P(1)	2.2411(18)	N(1)-Cu(1)-P(1)	112.57(18)
Cu(1)-N(2)	2.123(6)	N(2)-Cu(1)-P(1)	117.37(17)
Cu(1)-N(1)	2.095(6)	N(2)-Cu(1)-N(1)	80.3(2)
Cu(1)-N(3)	1.941(9)	N(3)-Cu(1)-P(1)	115.0(3)
Cu(2)-P(2)	2.2372(19)	N(3)-Cu(1)-N(1)	107.9(3)
Cu(2)-N(7)	2.095(6)	N(3)-Cu(1)-N(2)	117.9(3)
Cu(2)-N(6)	2.123(7)	N(7)-Cu(2)-P(2)	116.62(17)
Cu(2)-N(8)	1.943(8)	N(7)-Cu(2)-N(6)	79.5(2)
		N(6)-Cu(2)-P(2)	116.29(17)
		N(8)-Cu(2)-P(2)	115.1(2)
		N(8)-Cu(2)-N(7)	112.0(3)
		N(8)-Cu(2)-N(6)	112.5(3)
			Dihedral Angle
		P1-Cu1-N3/N1-Cu1-N2	87.516
		P2-Cu2-N8/N6-Cu2-N7	90.423

3

Cu(1)-P(1)	2.2505(6)	P(1)-Cu(1)-P(2)	107.55(2)
Cu(1)-P(2)	2.2563(6)	N(1)-Cu(1)-P(2)	121.45(5)
Cu(1)-N(1)	2.0689(18)	N(1)-Cu(1)-P(1)	112.39(5)
Cu(1)-N(2)	2.0673(18)	N(2)-Cu(1)-P(2)	116.32(5)
		N(2)-Cu(1)-P(1)	115.92(5)
		N(1)-Cu(1)-N(2)	81.81(7)
			Dihedral Angle
		P1-Cu1-P2/N1-Cu1-N2	86.407

4

Cu(1)-P(1)	2.2537(6)	P(2)-Cu(1)-P(1)	107.77(2)
Cu(1)-P(2)	2.2518(6)	N(1)-Cu(1)-P(2)	115.96(5)
Cu(1)-N(1)	2.0664(17)	N(1)-Cu(1)-P(1)	116.61(5)
Cu(1)-N(2)	2.0672(17)	N(2)-Cu(1)-N(1)	81.87(7)
		N(2)-Cu(1)-P(2)	112.01(5)
		N(2)-Cu(1)-P(1)	121.15(5)
			Dihedral Angle
		P1-Cu1-P2/N1-Cu1-N2	86.441

5

Cu(1)-P(1)	2.2304(5)	P(1)-Cu(1)-P(2)	104.855(19)
Cu(1)-P(2)	2.2417(5)	N(2)-Cu(1)-P(1)	110.65(4)
Cu(1)-N(1)	2.0606(16)	N(2)-Cu(1)-P(2)	114.28(5)

Cu(1)-N(2)	2.0710(15)	N(1)-Cu(1)-P(1)	116.30(4)
		N(1)-Cu(1)-P(2)	127.07(5)
		N(2)-Cu(1)-N(1)	81.48(6)
			Dihedral Angle
		P1-Cu1-P2/N1-Cu1-N2	91.822
6			
Cu(1)-N(3)	2.054(4)	N(3)-Cu(1)-N(4)	80.70(15)
Cu(1)-N(4)	2.061(3)	N(3)-Cu(1)-P(1)	127.51(11)
Cu(1)-P(1)	2.2327(12)	N(3)-Cu(1)-P(2)	116.18(10)
Cu(1)-P(2)	2.2239(14)	N(4)-Cu(1)-P(1)	115.06(10)
		N(4)-Cu(1)-P(2)	110.46(12)
		P(2)-Cu(1)-P(1)	104.67(5)
			Dihedral Angle
		P1-Cu1-P2/N3-Cu1-N4	91.551

Table S3 Intermolecular π - π interactions for complex **1**.

	Cg→Cg	Distance / Å	Slippage / Å
1	Cg(20)→Cg(20) ⁱ	3.698(7)	1.442

Cg(20) = N1-C2-C3-C4-C5-C6

Symmetric codes: ⁱ 1-x, 1-y, 1-z

Table S4 Intermolecular C-H \cdots π interactions for complex **2**.

	C-H→Cg	H \cdots Cg / Å	C-H \cdots Cg / °	C \cdots Cg / Å	C-H \cdots π / °
2	C9-H9→Cg(10) ⁱ	2.89	146	3.7188	68

Cg(10) = C23-C24-C25-C26-C27-C28

Symmetric codes: ⁱ -1+x, y, z

Table S5 Intermolecular π - π interactions for complex **3**.

	Cg→Cg	Distance / Å	Slippage / Å
3	Cg(3)→Cg(3) ⁱ	3.6114	1.442

Cg(3) = N1-C1-C2-C3-C4-C5

Symmetric codes: ⁱ 1/2-x, 1/2-y, 1/2-z

Table S6 Intermolecular C-H \cdots π interactions for complex **3**.

	C-H→Cg	H \cdots Cg / Å	C-H \cdots Cg / °	C \cdots Cg / Å	C-H \cdots π / °
3	C11-H11→Cg(9) ⁱ	2.70	155	3.569(2)	72
	C20-H20A→Cg(5) ⁱⁱ	2.97	139	3.758(3)	34
	C31-H31→Cg(9) ⁱⁱⁱ	2.97	161	3.859(3)	86

Cg(5) = N4-C15-C16-C19-C18-C17

Cg(9) = C34-C35-C36-C37-C38-C39

Symmetric codes: ⁱ 1/2-x, 1/2-y, 1/2-z; ⁱⁱ 1-x, 1-y, 1-z; ⁱⁱⁱ x, -1+y, z

Table S7 Typical hydrogen bonds in asymmetric units for complexes **3**.

	Hydrogen bonds	D-H / Å	H...A / Å	D...A / Å	D-H...A / °
3	C2-H2...F1 ⁱ	0.93	2.44	3.267(3)	149
	C19-H19...F4 ⁱⁱ	0.93	2.40	3.271(4)	155
	C20-H20B...F3 ⁱⁱⁱ	0.97	2.47	3.426(3)	168
	C33-H33A...F4 ⁱⁱⁱ	0.97	2.52	3.423(3)	156
	C35-H35...F3 ⁱⁱⁱ	0.93	2.49	3.378(3)	159
	C42-H42...F2	0.93	2.40	3.168(3)	140

Symmetric codes: ⁱ 1/2-x, 1/2-y, 1/2-z; ⁱⁱ 1/2-x, y, 1-z; ⁱⁱⁱ 1/2+x, 1-y, z**Table S8** Intermolecular π - π interactions for complex **4**.

	Cg→Cg	Distance / Å	Slippage / Å
4	Cg(4)→Cg(4) ⁱ	3.5841	1.404

Cg(4) = N2-C6-C7-C8-C9-C10

Symmetric codes: ⁱ 1/2-x, 3/2-y, 1/2-z**Table S9** Intermolecular C-H... π interactions for complex **4**.

	C-H→Cg	H...Cg / Å	C-H...Cg / °	C...Cg / Å	C-H... π / °
4	C12-H12→Cg(10) ⁱ	2.64	156	3.514(2)	70
	C20-H20B→Cg(5) ⁱⁱ	2.97	140	3.761(3)	35

Cg(10) = C40-C41-C42-C43-C44-C45

Cg(5) = N4-C15-C16-C17-C18-C19

Symmetric codes: ⁱ 1/2-x, 3/2-y, 1/2-z; ⁱⁱ 1-x, 1-y, 1-z**Table S10** Typical hydrogen bonds in asymmetric units for complexes **4**.

	Hydrogen bonds	D-H / Å	H...A / Å	D...A / Å	D-H...A / °
4	C9-H9...O4 ⁱ	0.93	2.50	3.319(3)	147
	C17-H17...O1 ⁱⁱ	0.93	2.46	3.316(4)	154
	C20-H20A...O2	0.97	2.54	3.496(4)	168
	C33-H33B...O1	0.97	2.54	3.443(3)	155
	C36-H36...O3 ⁱⁱⁱ	0.93	2.44	3.182(3)	137
	C45-H45...O2	0.93	2.57	3.456(3)	159

Symmetric codes: ⁱ 1-x, 1/2+y, 1/2-z; ⁱⁱ 1-x, 1-y, 1-z; ⁱⁱⁱ -1/2+x, 1-y, z**Table S11** Intermolecular π - π interactions for complex **5**.

	Cg→Cg	Distance / Å	Slippage / Å
5	Cg(6)→Cg(6) ⁱ	3.7476	1.722

Cg(4) = C4-C5-C6-C7-C12-C11

Symmetric codes: ⁱ 1-x, 2-y, 1-z**Table S12** Intermolecular C-H... π interactions for complex **5**.

	C-H→Cg	H...Cg / Å	C-H...Cg angle / °	C...Cg distance / Å	C-H... π / °
--	--------	------------	--------------------	---------------------	------------------

5	C8-H8→Cg(10) ⁱ	2.94	153	3.813(2)	72
	C13-H13B→Cg(5) ⁱⁱ	2.99	114	3.514(2)	25

Cg(10) = 38-C39-C40-C41-C42-C43

Cg(5) = N4-C15-C16-C17-C18-C19

Symmetric codes: ⁱ 1-x, 2-y, 1-z; ⁱⁱ 2-x, 1-y, -z

Table S13 Typical hydrogen bonds in asymmetric units for complexes **5**.

Hydrogen bonds	D-H / Å	H...A / Å	D...A / Å	D-H...A / °
5 C1-H1...F1	0.95	2.32	3.264(2)	173
C3-H3...F4 ⁱ	0.95	2.24	3.075(4)	147
C10-H10...F2 ⁱⁱ	0.95	2.49	3.297(3)	143
C13-H13A...F1	0.99	2.49	3.432(2)	158
C14-H14B...F1	0.99	2.49	3.422(2)	157
C29-H29...F1 ⁱⁱⁱ	0.95	2.53	3.466(3)	168
C34-H34...F3 ⁱⁱ	0.95	2.36	3.287(3)	166

Symmetric codes: ⁱ 2-x, 2-y, 1-z; ⁱⁱ -1+x, y, z; ⁱⁱⁱ 2-x, 1-y, 1-z

Table S14 Intermolecular π - π interactions for complex **6**.

	Cg→Cg	Distance / Å	Slippage / Å
6 Cg(10)→Cg(10) ⁱ		3.749(3)	1.652

Cg(4) = C35-C36-C37-C38-C43-C42

Symmetric codes: ⁱ 2-x, 1-y, -z

Table S15 Typical hydrogen bonds in asymmetric units for complexes **6**.

Hydrogen bonds	D-H / Å	H...A / Å	D...A / Å	D-H...A / °
6 C2-H2B...O2	0.97	2.55	3.486(6)	162
C18-H18...O1 ⁱ	0.93	2.55	3.453(9)	163
C32-H32...O3 ⁱ	0.93	2.53	3.324(7)	143
C39-H39...O4 ⁱⁱ	0.93	2.37	3.176(10)	145
C41-H41...O2	0.93	2.37	3.303(7)	175

Symmetric codes: ⁱ 1+x, y, z; ⁱⁱ 1-x, 1-y, -z

Table S16. Energy, oscillator strength and major contribution of the calculated transitions for **1-6**.

Excited state	Energy / eV (/ nm)	Oscillator strength	Major contribution (%)
1 absorption	4.8393 (256.20)	0.0987	HOMO-26→LUMO+2 (2.73)
			HOMO-25 → LUMO (3.36)
			HOMO-16 → LUMO+2 (2.56)
			HOMO-14 → LUMO+6 (8.36)
			HOMO-14 → LUMO+7 (3.83)
			HOMO-13 → LUMO+4 (2.51)
			HOMO-13 → LUMO+5 (30.78)

			HOMO-13 → LUMO+8 (12.08)
			HOMO-10 → LUMO+13 (2.48)
1	emission	2.0756 (597.34)	0.0251
			HOMO-9 → LUMO+1 (2.07)
			HOMO-7 → LUMO (5.04)
			HOMO-7 → LUMO+1 (3.63)
			HOMO-6 → LUMO (39.15)
			HOMO-5 → LUMO (3.18)
			HOMO-4 → LUMO (40.71)
			HOMO-2 → LUMO (3.31)
2	absorption	4.7933 (258.66)	0.1715
			HOMO-28 → LUMO+1 (3.56)
			HOMO-27 → LUMO+1 (12.19)
			HOMO-26 → LUMO+1 (5.35)
			HOMO-24 → LUMO+2 (6.92)
			HOMO-24 → LUMO+3 (2.98)
			HOMO-23 → LUMO+1 (12.93)
			HOMO-22 → LUMO+1 (7.11)
			HOMO-21 → LUMO+1 (4.41)
			HOMO-20 → LUMO+1 (3.61)
			HOMO-19 → LUMO+1 (8.75)
			HOMO-19 → LUMO+3 (2.37)
			HOMO-13 → LUMO+3 (6.97)
			HOMO-6 → LUMO+12 (2.90)
2	emission	3.3366 (530.61)	0.0270
			HOMO-8 → LUMO (3.18)
			HOMO-8 → LUMO+1 (7.00)
			HOMO-7 → LUMO (33.23)
			HOMO-6 → LUMO (39.30)
			HOMO-5 → LUMO (9.50)
			HOMO-4 → LUMO (3.78)
3	4	4.8558 (255.33)	0.1706
	absorption		
			HOMO-16 → LUMO (17.51)
			HOMO-14 → LUMO+1 (2.91)
			HOMO-11 → LUMO+1 (2.54)
			HOMO-9 → LUMO+2 (2.30)
			HOMO-3 → LUMO+3 (12.02)
			HOMO-2 → LUMO+5 (17.06)
			HOMO-1 → LUMO+10 (15.45)
			HOMO-1 → LUMO+11 (9.06)
3	4	2.3920 (518.32)	0.1144
	emission		
			HOMO-1 → LUMO (98.00)
5	6	4.6879 (264.48)	0.1386
	absorption		
			HOMO-15 → LUMO (21.55)
			HOMO-15 → LUMO+1 (2.80)
			HOMO-12 → LUMO+1 (4.50)
			HOMO-5 → LUMO+1 (4.15)
			HOMO-4 → LUMO+1 (6.30)
			HOMO-3 → LUMO+2 (10.06)

				HOMO-2 → LUMO+5	(20.45)
				HOMO → LUMO+11	(10.66)
5	6	2.5319	0.0198	HOMO-3 → LUMO	(8.03)
emission	(489.69)			HOMO-2 → LUMO	(28.55)
				HOMO-1 → LUMO	(59.20)

Table S17. Calculated molecular frontier orbital energy / eV for **1-6**.

Frontier orbital	1	2	3 and 4	5 and 6
HOMO-29	-7.473	-7.532	-11.858	-11.849
HOMO-28	-7.411	-7.524	-11.810	-11.807
HOMO-27	-7.329	-7.495	-11.758	-11.761
HOMO-26	-7.305	-7.493	-11.626	-11.665
HOMO-25	-7.267	-7.390	-11.549	-11.520
HOMO-24	-7.234	-7.332	-11.462	-11.331
HOMO-23	-7.197	-7.308	-11.341	-11.256
HOMO-22	-7.155	-7.267	-11.307	-11.125
HOMO-21	-7.087	-7.220	-11.254	-10.983
HOMO-20	-7.051	-7.187	-11.174	-10.965
HOMO-19	-6.974	-7.164	-10.947	-10.933
HOMO-18	-6.951	-7.111	-10.344	-10.418
HOMO-17	-6.847	-7.019	-9.824	-9.909
HOMO-16	-6.797	-7.000	-9.812	-9.731
HOMO-15	-6.737	-6.863	-9.637	-9.576
HOMO-14	-6.436	-6.808	-9.575	-9.542
HOMO-13	-6.399	-6.790	-9.519	-9.516
HOMO-12	-6.328	-6.246	-9.478	-9.457
HOMO-11	-6.276	-6.217	-9.421	-9.426
HOMO-10	-5.930	-6.206	-9.362	-9.389
HOMO-9	-5.870	-6.142	-9.362	-9.351
HOMO-8	-5.792	-6.131	-9.343	-9.300
HOMO-7	-5.687	-6.058	-9.312	-9.288
HOMO-6	-5.588	-5.785	-9.263	-9.248
HOMO-5	-5.114	-5.457	-9.247	-9.225
HOMO-4	-5.029	-5.427	-9.149	-9.059
HOMO-3	-5.001	-5.417	-8.694	-8.697
HOMO-2	-4.952	-5.329	-8.540	-8.451
HOMO-1	-4.898	-5.149	-7.922	-7.931
HOMO	-4.825	-5.012	-7.842	-7.857
LUMO	-2.191	-2.220	-4.696	-4.524
LUMO+1	-2.154	-2.144	-4.573	-4.304
LUMO+2	-2.047	-2.097	-3.404	-3.381
LUMO+3	-2.011	-2.029	-3.224	-3.174
LUMO+4	-1.154	-1.128	-3.128	-3.157

LUMO+5	-1.050	-1.012	-2.990	-3.075
LUMO+6	-0.901	-0.920	-2.921	-3.011
LUMO+7	-0.874	-0.838	-2.889	-2.956
LUMO+8	-0.805	-0.822	-2.755	-2.827
LUMO+9	-0.804	-0.756	-2.732	-2.682
LUMO+10	-0.691	-0.711	-2.652	-2.628
LUMO+11	-0.675	-0.595	-2.530	-2.469
LUMO+12	-0.550	-0.424	-2.398	-2.418
LUMO+13	-0.447	-0.376	-2.145	-2.198
LUMO+14	-0.322	-0.259	-2.050	-1.939
LUMO+15	-0.217	-0.243	-1.631	-1.648
LUMO+16	-0.193	-0.188	-1.396	-1.426
LUMO+17	-0.137	-0.103	-1.360	-1.151
LUMO+18	0.512	0.528	-1.082	-1.117
LUMO+19	0.548	0.617	-0.963	-1.053
LUMO+20	0.660	0.668	-0.922	-0.940
LUMO+21	0.678	0.766	-0.853	-0.798
LUMO+22	0.834	0.867	-0.742	-0.749
LUMO+23	0.947	0.970	-0.622	-0.710
LUMO+24	1.001	1.048	-0.560	-0.649
LUMO+25	1.105	1.068	-0.438	-0.431
LUMO+26	1.119	1.099	-0.371	-0.363
LUMO+27	1.137	1.131	-0.303	-0.275
LUMO+28	1.222	1.216	-0.196	-0.223
LUMO+29	1.298	1.333	-0.123	-0.188
